COMPARATIVE ANALYSIS OF ALTERNATIVE IN-DOOR CALIBRATION TECHNIQUES FOR OFF-THE-SHELF DIGITAL CAMERAS

Ivan Detchev, Axel Ebeling, Ayman Habib
Department of Geomatics Engineering, University of Calgary,
2500 University Drive NW, Calgary, Alberta, T2N 1N4, CANADA
i.detchev@ucalgary.ca, aebeling@ucalgary.ca, ahabib@ucalgary.ca

ABSTRACT

With the decreasing price of electronics, more and more consumer grade or off-the-shelf digital cameras are flooding the market. This makes their use in close-range photogrammetric applications an inexpensive and convenient task. However, in order to be trusted for high quality object space reconstruction, these cameras must go through a calibration procedure. The purpose of this research project is to present a simple and practical way of performing camera calibration, so that the cost of the calibration will be proportional to the cost of the camera. With this concept in mind, a planar calibration board was built, and its targets were surveyed in two different ways. Several bundle adjustments were run in order to test the adequacy for the lens distortion model used, study the effects of using linear features as observations, and check the equivalency of using control points against distance constraints when defining the datum.

INTRODUCTION

Photogrammetry is the art and science of performing accurate reconstruction of 3D objects photographed in multiple 2D images. In traditional photogrammetry, special metric cameras are used for both aerial and close-range applications. They are specifically designed for mapping purposes, and their calibration is performed by dedicated organizations, where trained professionals ensure that high calibration quality is upheld. In fact, a proper camera calibration is one of the most essential aspects of pre-mission quality assurance procedures. However, in the recent past, more and more off-the-shelf digital cameras are flooding the market, and they have become a convenient and an inexpensive alternative for close-range photogrammetric applications such as structural deformation monitoring, cultural heritage documentation, face recognition, biomedical imaging, and many others. Since there is a very wide spectrum of such consumer grade off-the-shelf digital cameras, it has become more practical for the data providers to perform their own calibrations. The shift of such a complex task to the hands of the data providers mandates the development of simple and effective procedures for camera calibration. These procedures should also incur minimal expenditure, so that the cost of the calibration is proportional to the one of the camera being calibrated.

In photogrammetric literature the term camera calibration refers to specifically solving for the interior orientation parameters (IOPs) of a specific camera, not only the focal length or position and orientation in space. Generally, the precision of the estimated IOPs during the camera calibration procedure mainly depends on the camera station geometry (such that any potentially correlated parameters will decoupled as much as possible), the precision of image coordinate measurements, and the method of datum definition (Clarke and Fryer, 1998; Fraser, 1997). This paper will first go through some basic concepts related to camera calibration, and then it will explain the design of an easy-to-establish test field for the purposes of automated in-door camera calibration. The paper will also examine the adequacy of choice for a lens distortion model, i.e. is it necessary to solve for all the radial, decentric, and affine distortion parameters or is it sufficient to only solve for the first radial lens distortion coefficient? It will then investigate the equivalency of the resulting IOP sets for different calibration techniques: using point features against using point and line features as observations in the bundle adjustment, and using pre-surveyed control points against using distance constraints in order to define the datum. The equivalency of the different calibration results will be evaluated by comparing the bundles of light rays defined by the corresponding IOPs in image space. The bundle similarity method used in this paper is referred to as ROT, as it allows for relative rotations between the two bundles that are compared (Habib *et al.*, 2005).

CAMERA CALIBRATION BASICS

For camera calibration, a bundle adjustment with self-calibration is commonly used to solve for the desired IOPs, the exterior orientation parameters (EOPs) of the images involved, and for the object space coordinates of any tie points. The IOPs include the offset of the principal point, the principal distance, and the distortion parameters in image space. The EOPs include the location of the perspective centres and the orientation of the cameras with respect to the object space coordinate system. The observations involved are the image coordinates of the measured calibration targets. The mathematical model for a photogrammetric bundle adjustment is the collinearity equations (Kraus, 1993):

$$x = x_P - c \cdot \frac{r_{11} \cdot (X - X_0) + r_{21} \cdot (Y - Y_0) + r_{31} \cdot (Z - Z_0)}{r_{13} \cdot (X - X_0) + r_{23} \cdot (Y - Y_0) + r_{33} \cdot (Z - Z_0)} + \Delta x$$

$$(1)$$

$$y = y_P - c \cdot \frac{r_{12} \cdot (X - X_0) + r_{22} \cdot (Y - Y_0) + r_{32} \cdot (Z - Z_0)}{r_{13} \cdot (X - X_0) + r_{23} \cdot (Y - Y_0) + r_{33} \cdot (Z - Z_0)} + \Delta y$$

where:
- (x, y) are the observed image coordinates
- (x_P, y_P) are the principal point coordinates
- c is the principal distance
- r_{11} to r_{33} are the elements of the 3D rotation matrix based on the ω, φ, and κ angles
- (X, Y, Z) are the object coordinates of reconstructed tie points
- (X_0, Y_0, Z_0) are the object coordinates of camera perspective centres
- $(\Delta x, \Delta y)$ are the distortions in image space.

The distortions in the images space may be divided into radial lens distortion, decentric lens distortion, affine deformation, and others. There are many existing mathematical models, which attempt to describe these deviations from the collinearity conditions. Some examples are the Brown-Conrady model (Brown, 1971), the USGS simultaneous multiframe analytical calibration (SMAC) (Light, 1992), and the Chebyshev normalized orthogonal polynomials model (Smith *et al.*, 1992). The model used in this research is the following (Kraus, 1997):

$$\Delta x = k_1 \cdot (r^2 - r_0^2) \cdot x' + k_2 \cdot (r^4 - r_0^4) \cdot x' + p_1 \cdot (r^2 + 2 \cdot (x')^2) + 2 \cdot p_2 \cdot x' \cdot y' - a_1 \cdot x' + a_2 \cdot y'$$

$$(2)$$

$$\Delta y = k_1 \cdot (r^2 - r_0^2) \cdot y' + k_2 \cdot (r^4 - r_0^4) \cdot y' + p_2 \cdot (r^2 + 2 \cdot (y')^2) + 2 \cdot p_1 \cdot x' \cdot y' + a_1 \cdot y'$$

where:
- k_1 and k_2 are the radial lens distortion parameters
- p_1 and p_2 are the decentric lens distortion parameters
- a_1 and a_2 are the affine deformation parameters
- r is the radial distance, $r^2 = (x')^2 + (y')^2$, and $x' = x - x_P$, and $y' = y - y_P$
- r_0 is the radial distance with the least radial lens distortion.

In-door test fields for calibrating close-range photogrammetric cameras can be either 2D or 3D (see Figure 1). Examples for a 2D test field are a single wall in a room or a portable flat board. Examples for a 3D test field are an inside corner of a room, a cube or a cage.

In order to achieve an overall strong solution, the geometry of the camera stations during the image acquisition has to be taken under serious consideration, especially in cases when using a 2D test field. It is preferred that the bundles of light rays from the cameras to the calibration targets intersect at an angle as close as possible to 90º in both the horizontal (i.e. between left and right camera stations) and vertical (i.e. between the low and high camera stations) planes (see
Figure 2 for a visual illustration in the case of a 2D test field). Ideally, all targets should be present in all images and the image format should be filled with targets as much as possible. Also, photographs in both landscape and portrait orientation must be taken in order to decouple the IOPs and EOPs (Remondino and Fraser, 2006).
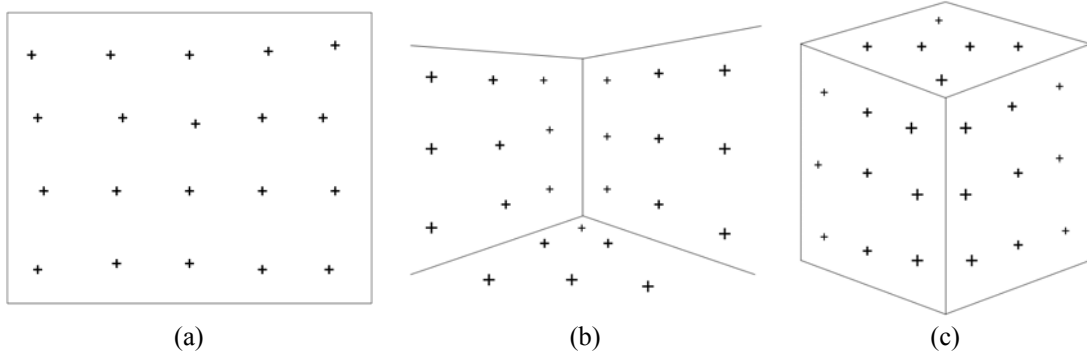
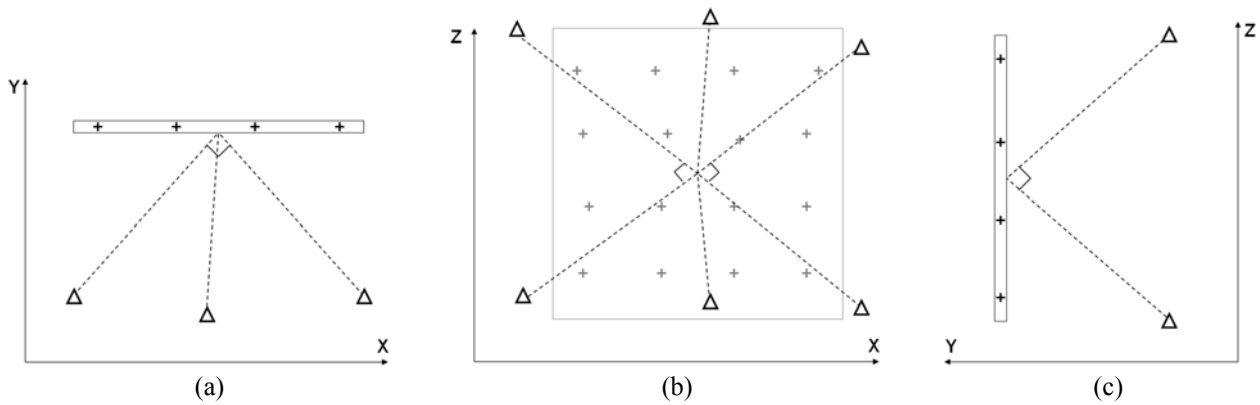**Figure 1.** Examples of 2D (a), and 3D (b-c) calibration test fields.

Figure 2. Top (a), front (b), and side (c) views of the configuration of camera stations (triangles) with respect to the calibration targets (crosses).

Other factors for a successful camera calibration are the image measurement precision and the way the datum for the object space coordinate system is defined. The image measurement precision depends on whether natural or signalized targets are used, and whether the targets are measured manually or automatically. Some examples of signalized targets are crosses, circles or checker-board squares (see Figure 3).
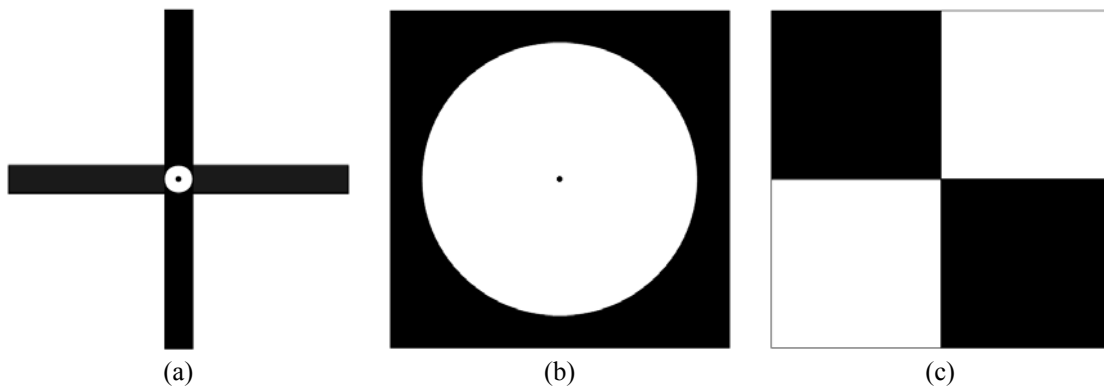

Figure 3. Examples of cross (a), circle (b), and checker-board (c) signalized targets.

The datum can be defined by either using pre-surveyed control points or by fixing the object coordinates of certain points and using distance constraints. The control points or distance measurement must be well distributed and encompass the entire image as much as possible (see
Figure 4 for visual examples). In all cases, tie points are necessary to increase the redundancy and strengthen the bundle adjustment solution.
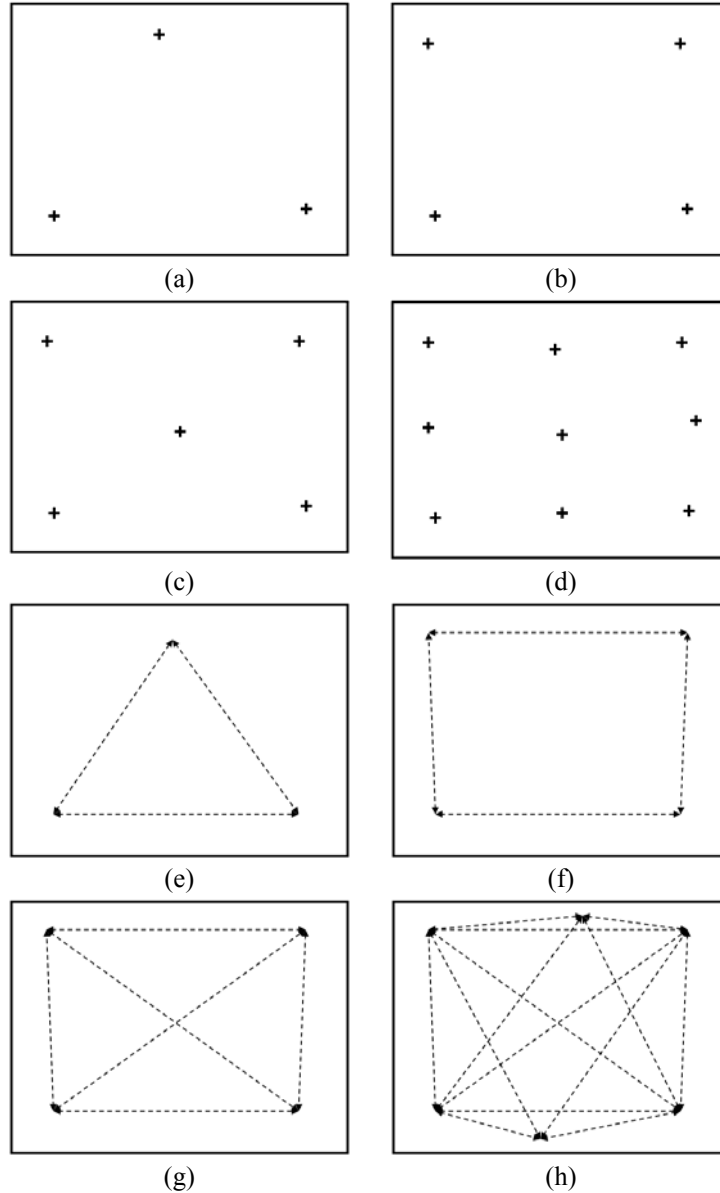

Figure 4. Examples of control point (a-d), and distance measurement (e-h) distribution in the image format.

PORTABLE CALIBRATION BOARD

The ideal option for a test field when calibrating close-range photogrammetric cameras is a 3D cage, i.e. the points observed fill up a 3D volume. However, it is very difficult and/or expensive to secure space that is large enough for such a calibration cage, so a 2D test field is often more convenient to have. Also, the target points within the test field need to be surveyed. Conventionally, this is done with specialized surveying instruments (e.g. a total station). Again, this could be quite an expensive procedure, because a competent survey crew

must be hired, and high grade equipment must be rented, so a less complex alternative to this is to measure distances between certain points in the test field with a measuring tape. To avoid high cost, this research project used an easy-to-establish test field for the purposes of an automated in-door calibration. The test field was comprised of a portable flat board (1.5m x 1.2m) with attached point targets and linear features (see
Figure 5). The choice of target design fell on the checkerboard one, because it was suitable for automatically detecting the target centres, and at the same time, it was practical when pointing and focusing on the targets with a total station. The board was built with common construction materials and tools. It was sturdy enough so that it does not warp, but at the same time it was light enough so that it could be moved from one location to another. Thus, its major advantages were its portability and compactness. In addition, it needed a moderate number of target points, because the linear features were used in the estimation of the lens distortion parameters. In absence of any distortion, straight features in object space should also appear straight in image space. Any deviation from straightness in image space was attributed to the lens distortion parameters (Habib and Morgan, 2003; Habib *et al.*, 2002).
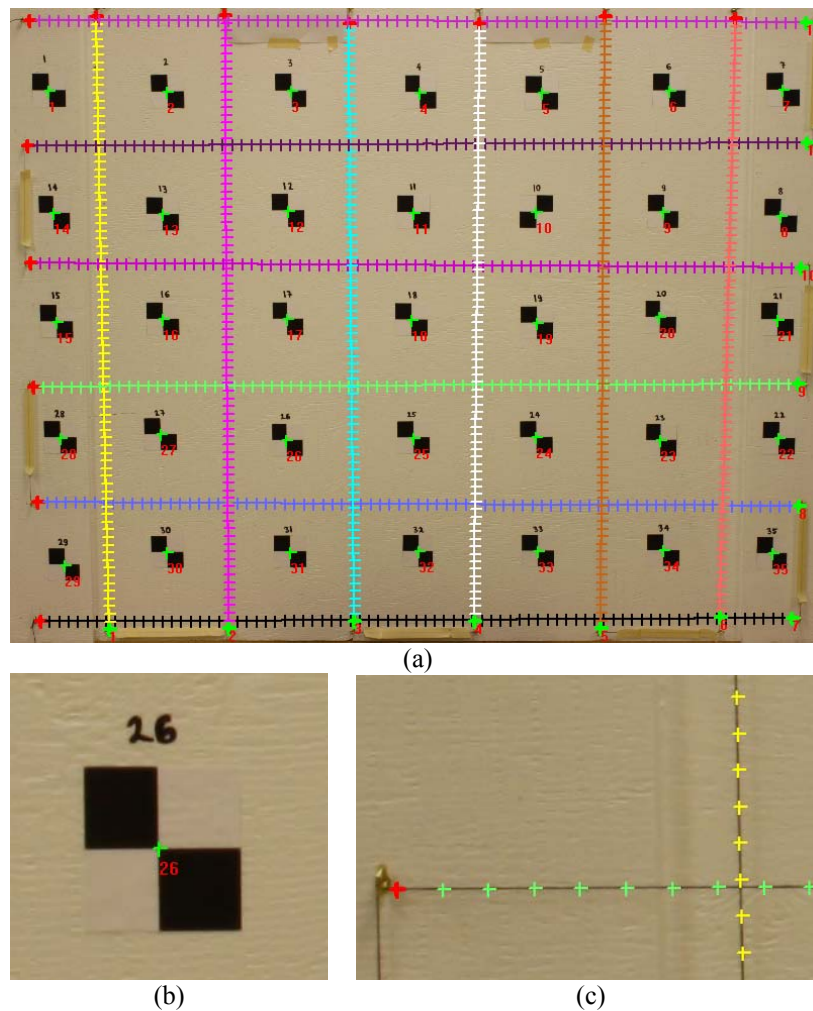

(a)

(b)

(c)

Figure 5. Example of a portable calibration board (a), with collected points (b) and linear features (c)

The linear features in image space were represented by two end points and a number of intermediate points along the line of interest. The mathematical constraint used in order to incorporate them as observations in the bundle adjustment followed the idea that the vector from the perspective centre to any intermediate image point is contained within the plane defined by the perspective centre of that image and the two points that define the straight line in object space (see Figure 6). The equation used was the following:

$$(\vec{V}_1 \times \vec{V}_2) \bullet \vec{V}_3 = 0 \tag{3}$$

where:
- the first vector connects the perspective centre to the first end point along the object space line
- the second vector connects the perspective centre to the second end point along the object space line
- the third vector connects the perspective centre to the intermediate point along the corresponding image line.

This constraint incorporates the image coordinates of any intermediate point, the EOPs, the IOPs (including the distortion parameters), and the ground coordinates of the points that define the object space line. Thus the constraint does not introduce any new parameters and it can be written for all intermediate points along each line in the imagery.
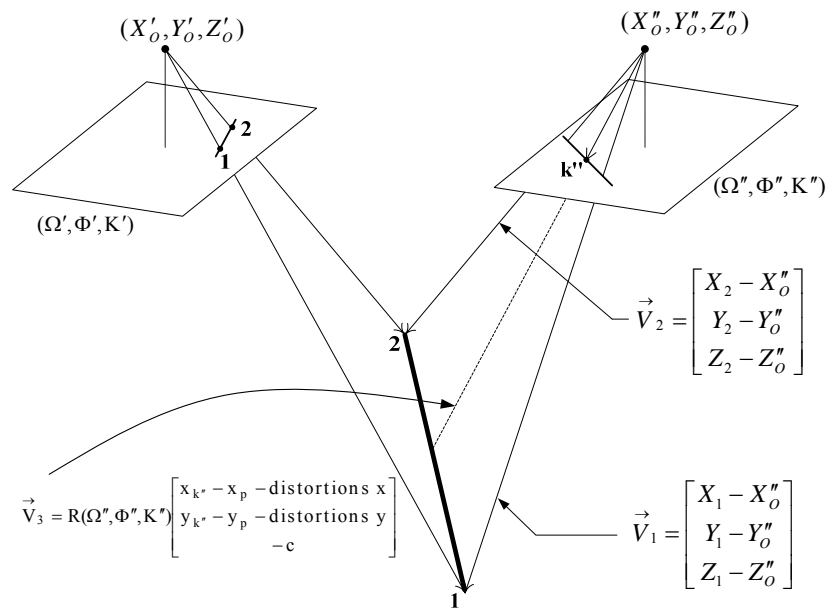

(X'_O, Y'_O, Z'_O)

(X''_O, Y''_O, Z''_O)

(Ω', Φ', K')

(Ω'', Φ'', K'')

$$\vec{V}_2 = \begin{bmatrix} X_2 - X''_O \\ Y_2 - Y''_O \\ Z_2 - Z''_O \end{bmatrix}$$

$$\vec{V}_3 = R(\Omega'', \Phi'', K'') \begin{bmatrix} x_{k''} - x_p - \text{distortions x} \\ y_{k''} - y_p - \text{distortions y} \\ -c \end{bmatrix}$$

$$\vec{V}_1 = \begin{bmatrix} X_1 - X''_O \\ Y_1 - Y''_O \\ Z_1 - Z''_O \end{bmatrix}$$

Figure 6. Perspective transformation between image and object space straight lines

ADEQUACY OF DISTORTION MODELS AND EQUIVALENCY OF INTERIOR ORIENTATION PARAMETER SETS

A lens distortion model can be categorized as inadequate, adequate or over-parameterized. An adequate model has the minimum number of distortion parameters needed to sufficiently describe the inherent distortions for the implemented camera. Insufficient and over-parameterized models should be avoided, because they might have an adverse effect on the reconstructed object space. The adequacy of lens distortion models used in bundle adjustment with self-calibration procedures can be evaluated by checking the a-posteriori standard deviations of the bundle adjustments (i.e. the overall precision values), by estimating the similarity between the bundles of light rays defined by the different IOP sets, and by checking the reconstruction accuracy in object space (i.e. performing a check point analysis). The bundle similarity method used in this paper will be the rotation one or ROT. In the ROT method two bundles of light rays share the same perspective centre, but they have different orientations in space, i.e. the two bundles are rotated to reduce the angular offset between conjugate light rays (see Figure 7). In order to evaluate the degree of similarity between the two bundles, a root mean square (RMS) value is computed. The RMS value represents the average spatial offset along the image plane between the conjugate light rays of the two bundles. The bundles are deemed similar if the computed RMS value is within the expected image measurement accuracy (e.g. half a pixel). In a similar manner, the ROT method is also used to investigate the equivalency of IOP sets resulted from different camera calibration techniques.
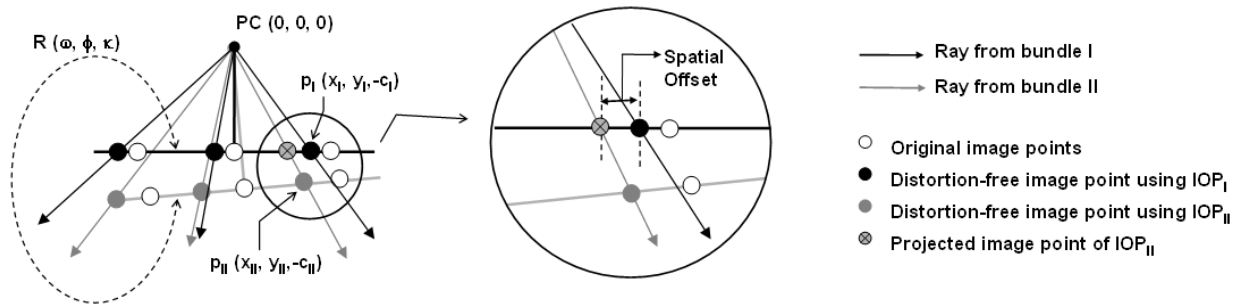
Figure 7. Visual representation of the ROT bundle similarity method.

EXPERIMENTAL RESULTS

The purpose of the experimental results was to investigate the differences between several combinations of camera calibration techniques. The first one was testing the necessity of solving for all the lens distortions as opposed to solving for only the first coefficient of radial lens distortion. The second one was using points only against using points and linear features as image space observations. Lastly, the third experiment was using control points against fixing the coordinates for a few points (in order to define the datum position and orientation) and using distance constraints (in order to define the datum scale). Before any of the experiments could be run, there were two data collection sessions.

The essence of first data collection session was to survey the targets on the portable calibration board. This was first done using a high precision total station, and two reflector prisms. According to manufacturer specifications, the measurement capabilities of the total station were 0.5" for the horizontal and vertical circle readings, and 1mm±1ppm for the electronic distance measurement (EDM) device. Note that the two reflector prisms have had their zero errors previously estimated. The observation points at which the total station was set up were two stable pillars. The portable target board was placed in such a way that the intersection angle between the directions from the two pillars was as close to 90º as possible. Horizontal directions, zenith angles, and slope distances from each pillar to the 35 target points on the board (and to the other pillar) were observed in two rounds. Each round involved both face left (direct), and face right (reverse) observations. The face left and face right observations were reduced for each round, and the two rounds were averaged after verifying that the observations were within the allowable discrepancies. After that, the averaged observations were fed into a surveying network adjustment in order to solve for the 3D coordinates of the target points. The standard deviations for the 3D coordinates were ±0.1mm for X, Y and Z. This method for surveying the target points was very cumbersome, and the combined time for data collection and processing took over two days. Another approach to survey the calibration board was to simply measure distances between selected points. Thus, ten distances between nine of the target points were measured using a construction quality tape measure, which had smallest graduation of 1mm. This was done twice by two different operators in order to avoid any reading blunders. The total time did not exceed 10-15 minutes, and the average of the differences in the distances measured with the tape measure and the ones calculated from the total station coordinates was 0.6mm with a standard deviation of ±0.3mm.

The second data collection session involved photographing the portable calibration board. The camera used was an entry level digital single-lens reflex (DSLR) one. The camera had a 22.2mm x 14.8mm complimentary metal oxide semiconductor (CMOS) solid state sensor. The output images had 3888 rows and 2592 columns or 10.1 effective megapixels, where the pixel size was 5.7μm. The camera lens had a nominal focal length of 35mm. The image stabilization, the automatic focus, and the sensor cleaning functions of the cameras were turned off to make sure they do not interfere with the calibration models. In addition, the zoom and focus rings were taped so that the focal length stayed fixed. Images were taken from three locations – left, centre, and right of the board. At each location, there was a low camera station (i.e. a tripod set at a height of 50cm), and a high camera station (i.e. a tripod set at a height of 180cm). At each camera station a landscape and a portrait orientation photos were taken (see Figure 8). Note that the origin of the coordinate system was chosen as the bottom left corner of the target board. Also, the three orthogonal set of lines at each exposure station represent the orientation of the cameras as defined by the ω, φ, and κ angles, i.e. the camera x-axis is in red, the y-axis in green, and the z-axis in blue.
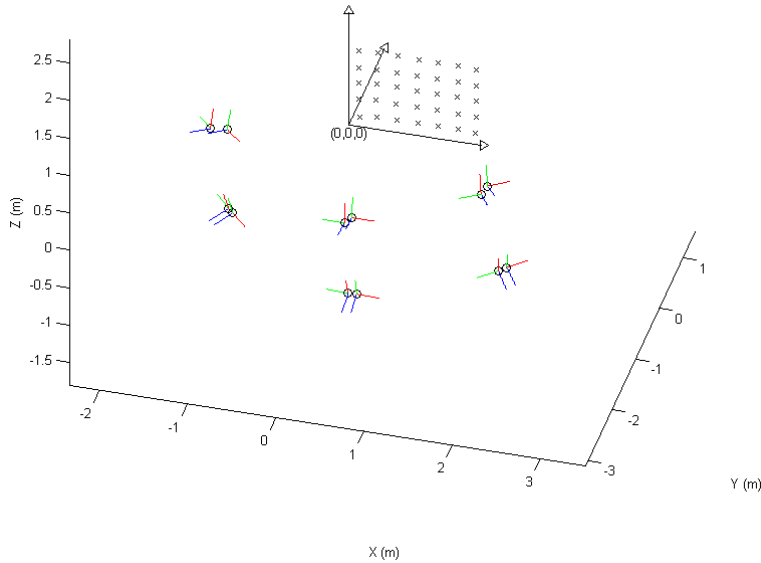
Figure 8. Camera calibration setup: camera stations (circles) and board targets (crosses).

The first test that was performed was to verify whether it is necessary to solve for all the lens distortion parameters, or to just use the first radial lens distortion coefficient (i.e. k_1) in the bundle adjustment with self-calibration. First, the adjustments were run with the surveyed points as the chosen control. The standard deviation used for each X, Y, Z coordinate was ±0.1mm. Then, the adjustments were run by fixing six coordinates (e.g. the X, Y, Z for one, the Y, Z for another, and the Y for a third point), and using the distances measured with the tape as control. The standard deviation used for all the distances was ±1mm.

Table 1. Differences in calibration results for using all six distortion parameters against using only k_1

	$\hat{\sigma}_o$ (µm) (all distortion parameters)	$\hat{\sigma}_o$ (µm) (only k_1)	ROT RMSE (µm)
Control points	0.9	1.1	1.4
Distance constraints	0.7	0.9	1.0

Table 2. RMSE between photogrammetric reconstruction and surveying measurements for calibration results when using all six distortion parameters against using only k_1

	Mean ΔX (mm)	Mean ΔY (mm)	Mean ΔZ (mm)	σ ΔX (mm)	σ ΔY (mm)	σ ΔZ (mm)	RMS X (mm)	RMS Y (mm)	RMS Z (mm)	Total RMSE (mm)
Distance constraints (all distortion parameters)	0.00	0.00	0.00	±0.09	±0.10	±0.05	0.09	0.10	0.05	**0.14**
Distance constraints (only k_1)	0.00	0.00	0.00	±0.11	±0.12	±0.06	0.11	0.11	0.06	**0.17**

The results from the first test were summarized in Table 1. If the a-posteriori standard deviations for the bundle adjustments using all six distortion parameters were compared against the bundles adjustments using only the k_1 parameter, it could be noticed that the differences were in the vicinity of 0.2µm (see first two columns in Table 1). This value was much less than the pixel size of 5.7µm, so the differences could be considered insignificant. Also, the calibration results for the two types of distortion models were regarded as equivalent, because the RMS values

between the bundles of light rays defined with all six distortion parameters and the ones defined with only k_1 were under half a pixel (see the last column in Table 1) regardless of whether the datum was defined by control points or with distance constraints. In addition, the object space reconstructions for the two distortion models only demonstrated differences at a level less than 0.1mm, i.e. less than what could be trustfully measured with the total station (see Table 2). Since solving for all six distortion parameters did not seem to be crucial, the rest of the experiments in this paper involved only solving for k_1.

Table 3. IOP differences for using control points only against using control points and linear features

	x_P (µm)	σx_P (µm)	y_P (µm)	σy_P (µm)	c (mm)	σc (µm)	k_1 (mm^{-2})	σk_1 (mm^{-2})	ROT RMSE (µm)
Control points only	-22.0	±4.0	-177.6	±4.4	34.902	±4.8	-1.70e-5	±6.45e-7	**0.9**
Control points (with linear features)	-21.4	±1.6	-186.5	±1.7	34.908	±2.1	-1.68e-5	±1.75e-7	

The second test was to perform a bundle adjustment with self-calibration using only points and points and linear features as observations in image space. Previous research had shown that including linear features as observations improved the standard deviations for the estimated IOPs (Habib and Morgan, 2005). The differences in the IOP results between the two adjustments for this experiment were summarized in Table 3. It could be noticed that the results were quite similar. In fact, the ROT RMSE between the bundles of light rays for both calibration results was 0.9µm, which deemed them equivalent. However, the IOPs for the latter solution do have better standard deviations. Also, so do the EOPs for the same solution. Most likely, the reason for this was that, because more observations were used in the least squares adjustment, the redundancy was much higher. This test supported the finding previously published.

Table 4. IOP differences for using control points against using distance constraints

	x_P (µm)	σx_P (µm)	y_P (µm)	σy_P (µm)	c (mm)	σc (µm)	k_1 (mm^{-2})	σk_1 (mm^{-2})	ROT RMSE (µm)
Control points only	-22.0	±4.0	-177.6	±4.4	34.902	±4.8	-1.70e-5	±6.45e-7	**2.8**
Distance constraints	-20.7	±4.4	-191.5	±4.6	34.920	±4.8	-1.65e-5	±1.18e-6	
Control points (with linear features)	-21.4	±1.6	-186.5	±1.7	34.908	±2.1	-1.68e-5	±1.75e-7	**0.3**
Distance constraints (with linear features)	-21.6	±1.6	-188.0	±1.8	34.910	±2.1	-1.68e-5	±1.78e-7	

Table 5. RMSE between photogrammetric reconstruction and surveying measurements for calibration results when using points only against using points and linear features as observations

	Mean ΔX (mm)	Mean ΔY (mm)	Mean ΔZ (mm)	σ ΔX (mm)	σ ΔY (mm)	σ ΔZ (mm)	RMS X (mm)	RMS Y (mm)	RMS Z (mm)	Total RMSE (mm)
Distance constraints (w/out linear features)	0.00	0.00	0.00	±0.12	±0.12	±0.06	0.12	0.12	0.06	**0.17**
Distance constraints (w/ linear features)	0.00	0.00	0.00	±0.11	±0.12	±0.06	0.11	0.11	0.06	**0.17**

The third test was to perform a bundle adjustment with self-calibration using control points and using distance constraints in order to define the object coordinate datum. From the first two rows of Table 4, it could be noticed that there were some differences in the results, especially for the estimate of y_P and the principal distance, c.

However, the ROT RMSE between the bundles of light rays for these two sets of IOPs was 2.8μm, which was exactly half a pixel. Moreover, if linear features were added as observations in the image space (see last two rows of Table 4), the results from the two adjustments became almost identical with ROT RMSE of 0.3μm.

Even though using linear features as observables seemed to improve the standard deviations for the solved IOPs, it is worth mentioning that the quality of the 3D reconstruction for the board targets did not change. Table 5 lists the RMS values between the two photogrammetric reconstructions (using distance constraints without or with linear features) and the total station survey.

CONCLUSIONS AND RECOMMENDATIONS

This paper explored some variations in performing a bundle adjustment with self-calibration for a consumer grade camera. The aim of the experiments was to make the camera calibration process simpler and more practical. In order to save space and lower expenses, a portable and at the same time easy-to-build planar calibration board was used. The target points on the board were surveyed with both a high precision total station and with a construction quality measuring tape. The imagery was collected with convergent geometry and several bundle adjustments were run. The first finding was that it was not necessary to solve for all the six lens distortion parameters for the implemented camera, i.e. estimating only k_1 yielded an adequate set of IOPs – the bundle adjustment had sub-pixel level precision in image space, and sub-millimetre accuracy in object space. The second finding (or rather – confirmation) was that adding linear features to the calibration procedure seemed to improve the precision of the estimated IOPs (due to increased redundancy), but did not increase the accuracy in object space. The last finding was that whether control points or distance constraints were used to define the datum, the output IOP sets were equivalent, especially if linear features were used as observations. In conclusion – in the cases when using a portable size calibration board for the calibration of an off-the-shelf digital camera, it is more practical to measure the target points with a tape measure than with a total station. If there is available software to automatically collect linear features in image space, including them in the bundle adjustment is an added bonus. Future work will include applying the findings from this research in projects involving object space reconstruction such as structural deformation monitoring or biomedical imaging.

ACKNOWLEDGEMENTS

REFERENCES

Brown, D.C., 1971. Close-range camera calibration, *Photogrammetric Engineering & Remote Sensing*, 37(8): 855-866.

Clarke, T.A., and J.G. Fryer, 1998. The development of camera calibration methods and models, *Photogrammetric Record*, 16(91): 51-66.

Fraser, C.S., 1997. Digital camera self-calibration, *ISPRS Journal of Photogrammetry and Remote Sensing*, 52(4): 149-159.

Habib, A.F., and M.F. Morgan, 2003. Automatic calibration of low-cost digital cameras, *Journal of Optical Engineering*, 42(4): 948-955.

Habib, A.F., and M.F. Morgan, 2005. Stability analysis and geometric calibration of off-the-shelf digital cameras, *Photogrammetric Engineering & Remote Sensing*, 71(6): 733-741.

Habib, A.F., M.F. Morgan, and Y.-R. Lee, 2002. Bundle adjustment with self-calibration using straight lines, *Photogrammetric Record*, 17(100): 635-650.

Habib, A.F., A.M. Pullivelli, and M.F. Morgan, 2005. Quantitative measures for the evaluation of camera stability, *Journal of Optical Engineering*, 44(3): 033605.

Kraus, K., 1993. *Photogrammetry, volume 1: Fundamentals and standard processes*, Ferd. Duemmlers Verlag, Bonn, 397 p.

Kraus, K., 1997. *Photogrammetry, Volume 2: Advanced Methods and Applications*, Ferd. Duemmlers Verlag, Bonn, 466 p.

Light, D.L., 1992. The new camera calibration system at the U.S. Geological Survey, *Photogrammetric Engineering & Remote Sensing*, 58(2): 185-188.

Remondino, F., and C. Fraser, 2006. Digital camera calibration methods: Considerations and comparisons, *Proceedings of the ISPRS Commission V Symposium "Image Engineering and Vision Metrology"*, Volume XXXVI, Part 5, September 25-27, Dresden, Germany, pp. 266-272

Smith, W.E., N. Vakil, and S.A. Maislin, 1992. Correction of distortion in endoscopic images, *IEEE Transactions on Medical Imaging*, 11(1): 117-122.